

Development of a correlated-k distribution band model scheme for the radiative transfer program GOMETRAN/SCIATRAN for retrieval of atmospheric constituents from SCIAMACHY/ENVISAT-1 data

M. Buchwitz, V. V. Rozanov and J. P. Burrows

Institute of Remote Sensing (*ife*), University of Bremen,
P.O. Box 33 04 40, 28344 Bremen, Germany

ABSTRACT

GOMETRAN/SCIATRAN is a radiative transfer forward model developed for retrieval of atmospheric trace gas concentrations, aerosol and cloud parameters, and surface reflectance from the spectral radiance measurements of the SCIAMACHY/ENVISAT-1 and GOME/ERS-2 UV-Vis-NIR multi-channel spectrometers. For radiative transfer modeling of the line absorptions of O₂, H₂O, CO₂, CH₄, N₂O, and CO, two different schemes are under development: an accurate but rather slow line-by-line (LBL) implementation and a significantly faster correlated-*k* (*c-k*) distribution scheme. The *c-k* scheme has been matched to the resolution of the instruments, which is channel dependent. In spectral regions free of overlapping line-absorbers the multiply scattered radiance calculated with both, the LBL and the *c-k* scheme, agrees within 1-2%. Calculations in *c-k* mode are a factor of 25-800 faster depending on spectral interval. Good agreement has been found with the MODTRAN/DISORT radiative transfer model. First results concerning a new method are presented indicating that overlapping line-absorbers can be modeled with similar accuracy and speed as single line-absorbers.

Keywords: Radiative transfer, remote sensing, atmospheric chemistry, band model, k distribution, ESFT, SCIAMACHY, GOME, GOMETRAN

1. INTRODUCTION

A central part of almost any inversion algorithm aimed to retrieve geophysical information from remote sensing measurements is an accurate and fast forward model that relates the desired geophysical parameters with the directly measured quantities. GOMETRAN/SCIATRAN (GT/ST) is a radiative transfer (RT) forward model developed for the retrieval of geophysical parameters from the spectral UV-Vis-NIR radiance measurements of the SCanning Imaging Absorption spectroMeter for Atmospheric CHartography (SCIAMACHY)^{1 2} multi-channel spectrometer (240-2380 nm) and for the similar Global Ozone Monitoring Experiment (GOME)³ (240-790 nm). SCIAMACHY is expected to be launched on board the European Space Agency's (ESA) ENVISAT-1 satellite in the year 2000. GOME on ESA's ERS-2 satellite has successfully been delivering data since its launch in April 1995. SCIATRAN is an extension of the GOMETRAN RT model.^{4 5 6 7 8 9}

GT/ST has a unique capability especially important for atmospheric constituents retrieval: the so called weighting functions, i.e. the derivatives of the radiance with respect to atmospheric (fit) parameters, like trace gas concentration, pressure, temperature, and aerosol profiles as well as albedo, can be determined using a newly developed quasi-analytical approach⁵ thus avoiding the need to rely on time consuming numerical perturbation schemes. These weighting functions are needed by least-squares methods as, for example, the widely used optimal estimation scheme; a variant of this method has been successfully developed for ozone profile retrieval from GOME data.¹⁰

The topic of this paper is the modeling of line-absorbers in the UV-Vis-NIR spectral range within multiple scattering RT codes. A molecular gas absorber in this context is defined to be a line-absorber if its absorption cross-section can be calculated from spectroscopic line parameters such as line position, intensity, ground state energy

Other author information: (Send correspondence to M.B.)
M.B.: E-mail: Michael.Buchwitz@ife.physik.uni-bremen.de
V.V.R.: E-mail: Vladimir.Rozanov@ife.physik.uni-bremen.de
J.P.B.: E-mail: John.Burrows@ife.physik.uni-bremen.de

etc. Line-absorbers in the SCIAMACHY spectral range are O₂, H₂O, CO₂, CH₄, N₂O, and CO. The cross-section of line-absorbers generally show a strong dependence on wavelength, pressure, and temperature since individual lines can be spectrally resolved. In contrast the (UV-visible) absorption cross-section of continuum-absorbers show a rather smooth wavelength dependence compared with the spectral sampling of the instruments and generally a relatively weak dependence on pressure and temperature (for instance O₃ in the visible).

Two different schemes to model line-absorbers are under development for GT/ST. In addition to an accurate but slow line-by-line (LBL) implementation a correlated-*k* (*c-k*) distribution scheme is being developed to significantly reduce the computational burden of the forward model calculations in the retrieval process.

As the instrument's slit function full-width at half-maximum (FWHM) is larger than the width and the average distance between spectral lines, individual spectral lines are not resolved and, therefore, time consuming monochromatic (LBL) RT calculations are not required. What is needed are slit function averaged radiances. The method of choice for fast spectral mean radiance calculations within multiple scattering RT codes is the *c-k* approach.^{11 12 13 14} A specific implementation of this method, optimized for SCIAMACHY and GOME, is described in this paper focusing on three spectral regions: the H₂O overtone and combination vibration-rotation absorption bands around 720 nm, the O₂ A-band around 760 nm ($\Delta\nu = 0$ spin-forbidden $b^1\Sigma_g^+ \leftarrow X^3\Sigma_g^-$ electronic transition), and the 1435 nm spectral region containing strong overlapping H₂O and CO₂ (overtone and combination vibration-rotation) absorption bands. The backscattered radiances in the O₂ A-band provides important information on cloud parameters, such as cloud top height and coverage,¹⁵ and the 720 nm water bands are presently under investigation concerning water vapor total column retrieval from GOME (S. Noël, priv. communication).

A short description of the SCIAMACHY and GOME instruments is given in Section 2. The current status of the GT/ST RT model development is presented in Section 3. Sections 4 and 5 describe the LBL and the *c-k* distribution scheme in detail. A comprehensive comparison of both methods in terms of accuracy and computer time follows in Section 6. In Section 7 GT/ST radiances are compared with MODTRAN/DISORT^{16 17 18} radiance spectra.

2. THE SCIAMACHY AND GOME INSTRUMENTS

The SCIAMACHY instrument is a space-based spectrometer designed to measure the solar radiation scattered back and reflected by the Earth's atmosphere-surface system in the 240-2380 nm spectral region. SCIAMACHY is a national contribution to ESA's ENVISAT-1 satellite due for launch in late 1999 by Germany, the Netherlands, and Belgium. SCIAMACHY will observe scattered light in nadir and limb viewing geometries (global coverage) as well as transmitted light in solar and lunar occultation modes (mid- to high-latitudes). In addition the sun and the moon are observed directly mainly for calibration but also for scientific purposes.¹⁹

The spectral resolution of SCIAMACHY is about 0.2 nm (FWHM) in the UV (channels 1 and 2), 0.4 nm in the 400-1000 nm region (ch. 3-5), about 1.7 nm in the 1000-1750 nm near infrared (NIR) region covered by channel 6, and about 0.2 nm in the NIR channels 7 and 8 (1940-2040 nm and 2265-2380 nm, respectively). Each of the eight channels has a linear detector array comprising 1024 individual detector diodes.

SCIAMACHY has been designed to provide amounts and distributions of O₃, NO₂, BrO, SO₂, OClO, ClO, H₂CO, CO, CH₄, H₂O, N₂O, pressure, temperature, cloud parameters (e.g. cloud top height and cloud cover) and the solar irradiance as well as the earthshine radiance. A detailed description of the SCIAMACHY instrument, its scientific objectives, mission planning and calibration aspects, retrieval schemes and expected retrieval precisions can be found elsewhere.^{1 2 20 21}

GOME on ERS-2 is essentially a small scale version of SCIAMACHY limited to the nadir viewing mode and to the 240-790 nm spectral region. The first four channels of GOME and SCIAMACHY are essentially identical. A detailed description of the GOME instrument and its capabilities including operational and scientific data products can also be found elsewhere.³

3. THE GOMETRAN/SCIATRAN RADIATIVE TRANSFER MODEL

SCIATRAN is an extension of the GOMETRAN RT model.^{4 5 6 7 8} GT/ST solves the monochromatic scalar integro-differential RT equation in plane-parallel geometry:

$$\mu \frac{dI(z, \mu, \varphi)}{dz} = -\alpha(z)I(z, \mu, \varphi) + \frac{b(z)}{4\pi} \int_0^{2\pi} d\varphi' \int_{-1}^1 d\mu' p(z, \mu, \mu', \varphi, \varphi') I(z, \mu', \varphi'). \quad (1)$$

I denotes the full radiance field depending on spatial position (characterized by vertical coordinate z) and direction (characterized by μ , the cosine of the (polar or zenith) angle w.r.t. the vertical (z) direction, and φ , the relative azimuth angle w.r.t. the sun direction). α is the volume extinction coefficient (sum of absorption and scattering coefficient b), and $p(z, \mu, \mu', \varphi, \varphi')$ is the total scattering phase function (weighted sum of Rayleigh, aerosol and cloud phase functions) normalized to 4π , describing the fraction of the light scattered into direction (μ, φ) originally traveling along direction (μ', φ') . This equation including appropriate boundary conditions is solved by GT/ST using the *finite difference method*.⁴ One matrix equation is solved per wavelength for each Fourier component of the radiance field by LU matrix decomposition²² which is, in general, the most time consuming step in the forward simulation.

Spherical effects are approximated by calculating the solar source term in spherical geometry (“pseudo spherical approach”^{18 23}) including refraction. This gives accurate results for solar zenith angles (SZA) up to about 92° and for line-of-sight viewing angles close to nadir.

The latest version of GOMETRAN contains all relevant gas absorbers in the 240-2400 nm spectral range, Rayleigh scattering, two independent aerosol parameterizations ((i) the widely used LOWTRAN aerosol scheme²⁴ and (ii) a newly developed flexible “GOMETRAN aerosol parameterization” based on Mie calculations following WMO recommendations (R. Hoogen, J. Kauss, priv. communication), two cloud schemes,⁷ (i) an accurate but rather slow “clouds as layers” (CAL) scheme similar to the GOMETRAN aerosol model and (ii) a faster but approximative “clouds as reflecting boundary” (CAB) scheme. The Earth’s surface is presently considered to be a Lambertian reflector. Weighting functions, i.e. the derivatives of the radiance w.r.t. atmospheric and surface parameters, can be generated quasi-analytically for absorber concentration, pressure, temperature, and aerosol profiles, as well as for albedo.⁵ For the pressure and temperature weighting functions only the air density (pressure and temperature) and ozone UV cross-section (temperature) terms are considered at present. Rotational Raman (inelastic) scattering by air molecules can be modeled using an off-line version of GOMETRAN.⁹

The extension of GOMETRAN (covering GOME needs) to SCIATRAN (covering additional SCIAMACHY needs) mainly comprises the generation of appropriate data bases up to 2400 nm including c - k distribution band model parameters, as well as the development of a limb (spherical geometry) and occultation (transmittance) mode, including weighting functions, for atmospheric constituents retrieval from SCIAMACHY’s limb and solar and lunar occultation measurements.

4. LINE-BY-LINE (LBL) CALCULATIONS

LBL calculations are needed mainly for reference purposes. Any faster but generally less accurate alternative scheme has to be thoroughly compared with LBL results. In the following a description of the calculation of the monochromatic (pressure and temperature dependent) line-absorber cross-sections from spectroscopic line parameters and of the LBL scheme implementation is provided.

4.1. LBL absorption cross-section calculations

The pressure and temperature dependent absorption cross-section k at wavenumber ν for a single line is given by $k(\nu - \nu_o) = S(T) f(\nu - \nu_o)$. $S(T)$ is the line intensity at temperature T , f is the line shape function, and ν_o is the line center position. Usually several lines contribute to the cross-section at the wavelength/wavenumber of interest; these individual contributions have to be added together. The line intensity $S(T)$ at temperature T can be calculated from the line intensity $S_o := S(T_o)$ at reference temperature T_o as follows:

$$S(T) = S_o \frac{Q_o^\nu}{Q^\nu(T)} \frac{Q_o^r}{Q^r(T)} \exp \left[\frac{E_l}{k} \left(\frac{1}{T_o} - \frac{1}{T} \right) \right] \quad (2)$$

The stimulated emission term ($[1 - \exp(-h\nu/kT)]/[1 - \exp(-h\nu/kT_o)]$) has been neglected as this term is essentially unity (for SCIAMACHY ν is larger than 4000 cm^{-1} ($< 2400 \text{ nm}$) and kT corresponds to about 200 cm^{-1}

for atmospheric temperatures). The term $(Q_o^\nu/Q^\nu)(Q_o^r/Q^r)$ contains ratios of vibrational and rotational partition functions at the reference temperature T_o and the actual temperature T . The partition function term is calculated using the polynomial coefficients also stored in the HITRAN 96 data base. k is Boltzmann's constant, c is the speed of light, and h is Planck's constant.

The spectroscopic parameters used for the results presented in this paper are from the HITRAN 96 line data base.²⁵ The following line parameters are used in this study:

Line parameter	Comments	Unit
Position: ν_o	line center position	[cm ⁻¹]
Intensity: S_o	$T_o = 296$ K; isotope abundance weighted	[cm ⁻¹ (cm ² /molec.)]
Lower state Energy: E_l		[cm ⁻¹]
Air-broadened HWHM: γ_o^L	$T_o = 296$ K, $P_o = 1013$ hPa	[cm ⁻¹ /atm.]
Coeff. of T-depend. of γ_o^L : n	$\gamma^L = \gamma_o^L(p/p_o) (T_o/T)^n$	[-]

For all lines a Voigt line shape has been assumed which is essentially the convolution of a Lorentz line shape function (pressure broadening) with a Doppler line shape function (line broadening due to thermal motion):

$$f_V(\nu_o - \nu) = \int_{-\infty}^{+\infty} \frac{\gamma^L}{\pi} \sqrt{\frac{\tilde{m}}{2\pi kT}} \frac{1}{(\nu - \nu_o - \frac{u\nu_o}{c})^2 + (\gamma^L)^2} du \quad (3)$$

\tilde{m} is the molecular mass of the molecule of interest also part of the HITRAN 96 data base. γ^L is pressure and temperature dependent and can be obtained from γ_o^L and n by $\gamma^L = \gamma_o^L(p/p_o) (T_o/T)^n$.

4.2. Implementation of the GOMETRAN/SCIATRAN LBL mode

For each height level of the internal GT/ST altitude grid the monochromatic pressure and temperature dependent absorption cross-section of each line-absorber is calculated assuming a Voigt line shape²⁶ as described above. Only lines within a preselected wavenumber interval (usually 100 cm⁻¹) are considered to contribute to the wavelength of interest.

5. CORRELATED-K DISTRIBUTION (C-K) SCHEME

As SCIAMACHY and GOME do not resolve individual absorption lines spectral mean radiances rather than monochromatic radiances are required for retrieval. For mean transmittance calculations so called band models have been developed in order to parameterize the transmittance averaged over a finite spectral interval with only a small number of parameters. Certain band model schemes have been developed for dedicated spectral bands utilizing the statistics of line positions, intensities, etc. within these intervals. One band model approach, the so called *c-k* distribution method^{11 12 13 14} is especially suited for RT applications when absorption *and* multiple scattering is important. This method allows to interpret the band model parameters as absorption cross-sections, thus allowing the application of the Beer-Lambert law (even for mean transmittances and radiances) and, therefore, is compatible with the monochromatic structure of the underlying multiple scattering RT equation.

5.1. Description of the *c-k* method

5.1.1. Single line-absorber case

If only one line-absorber absorbs radiation in a given small spectral interval $\Delta\lambda$ all other wavelength dependent quantities like scattering and absorption cross-sections, phase functions, surface albedo, etc., might be considered *constant* in this interval. Therefore, the calculation of the mean transmittance or radiance for a homogeneous, i.e. constant pressure and temperature, path does not depend on the actual wavelength dependence of the line-absorber cross-section but only on its statistics, in the sense that only the fraction of the wavelength interval covered by cross-sections of a certain magnitude is of relevance. This means that the wavelength axis can be arbitrarily transformed. In the *c-k* method the (discretized) wavelength axis is transformed such that the cross-section *monotonically* increases (or stays constant) with respect to the new "wavelength" axis (usually denoted g). The sorted cross-section still may cover several orders of magnitude but is a rather *smooth* function w.r.t. g .

This transformation, i.e. the transformation $(\lambda, k_\lambda) \rightarrow (g, k_g)$, where k is the absorption cross-section of the line-absorber, enables the integral over the monochromatic transmittance $T_\lambda(m) = \exp(-k_\lambda m)$ (Beer-Lambert law) to be approximated by a finite sum with significantly less terms (here M) than would be required for the original highly structured k_λ (see Figure 1):

$$\langle T_\lambda(m) \rangle_{\Delta\lambda} := \frac{1}{\Delta\lambda} \int_{\lambda_f}^{\lambda_i} \exp(-k_\lambda m) d\lambda = \int_0^1 \exp(-k_g m) dg \approx \sum_{i=1}^M \omega_i \exp(-k_i m). \quad (4)$$

dg is the fraction of the wavelength interval $\Delta\lambda (= \lambda_f - \lambda_i)$ covered by absorption cross-sections between k and $k + dk$, i.e. $dg = f(k)dk$, where $f(k)$ is the cross-section distribution function (“ k distribution”). For each of the M g -subintervals a representative cross-section, k_i , might be found such that the corresponding transmittance $1/\Delta g_i \int_{\Delta g_i} \exp(-k_g m) dg$ can quite accurately be described by the usual Beer-Lambert law, i.e. $\exp(-k_i m)$. The approximate transmittance for the whole wavelength interval might then be obtained by adding the g -subinterval (Beer-Lambert law) transmittances with weights $\omega_i = \Delta g_i$, where Δg_i is the corresponding g -subinterval length. However, better fit parameters might be found by a suitable non-linear least squares (NLLS) fitting procedure that allows the minimisation of the NLLS residual R ,

$$R(M, \{\omega_i\}_{i=1..M}, \{k_i\}_{i=1..M}) := \sum_{n=1}^N \left[\langle T_\lambda(m_n) \rangle_{\Delta\lambda} - \sum_{i=1}^M \omega_i \exp(-k_i m_n) \right]^2, \quad (5)$$

for the whole wavelength interval simultaneously under the following constraints, which follow directly from the physical interpretation placed on these parameters (“cross-section”, “interval length”):

$$k_i \geq 0, \quad \omega_i > 0, \quad \sum_{i=1}^M \omega_i = 1. \quad (6)$$

As a sum of exponentials is fitted against a reference transmittance function this problem is usually referred to Exponential Sum Fitting of Transmittance functions (ESFT).²⁷ The band model parameters (or ESFT coefficients) k_i can be interpreted as effective absorption cross-sections for pseudo wavelength interval Δg_i . Therefore, this band model approach is compatible with a *monochromatic* multiple scattering code like GT/ST. If the mean radiance shall be calculated for wavelength interval $\Delta\lambda$ the RT equation simply has to be solved M times, each time for one of the M pseudo wavelength subintervals Δg_i for which the Beer Lambert law holds as in the monochromatic case. This gives M radiance values I_i . In order to obtain the desired mean radiance w.r.t. $\Delta\lambda$ the (pseudo) subinterval radiances simply have to be added according to:

$$\langle I_\lambda \rangle_{\Delta\lambda} = \sum_{i=1}^M \omega_i I_i. \quad (7)$$

A similar equation is valid for the weighting functions.

Unfortunately, for a vertically *inhomogeneous* atmosphere, as used in GT/ST, there is an additional problem: The *mapping* of the physical wavelength interval $\Delta\lambda$ into the pseudo wavelength interval g depends on pressure and temperature, i.e. the scrambling of the wavelength axis is not the same for different atmospheric levels. This results in errors because the wavelength coherence between the levels is disturbed. However, it might be a good approximation to assume that cross-sections for different pressures and temperatures are strongly wavelength correlated¹⁴ and, therefore, the wavelength transformations are nearly identical for all layers. The validity of this assumption, however, has to be carefully checked. The error introduced by applying the k distribution method to *inhomogeneous* atmospheres (correlated- k distribution method) has to be quantified by comparison with LBL calculations.

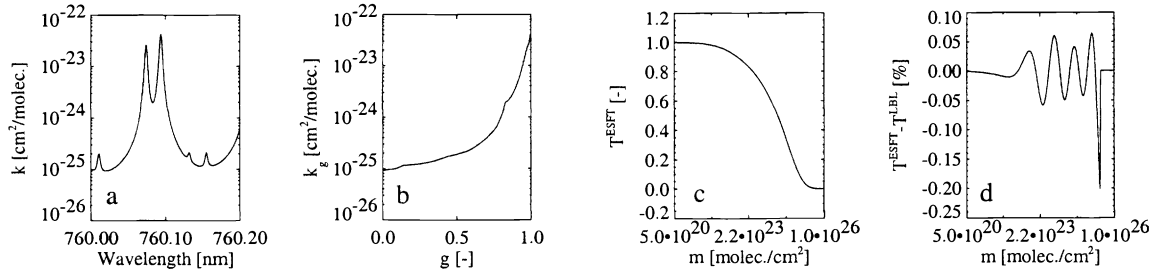


Figure 1. (a) Monochromatic O_2 absorption cross-section for a pressure of 500 mbar and a temperature of 250 K in a spectral interval corresponding to one detector pixel of GOME's and SCIAMACHY's channel 4 (0.2 nm pixel resolution). (b) The corresponding k -distribution. (c) ESFT transmittance ($M=10$), and (d) relative error between ESFT and LBL reference transmittance. Note that the error has been set to zero for transmittances less than 1% as the absolute transmittance error is negligible under these conditions. The r.m.s. deviation between the ESFT and the LBL transmittance is 0.035% ($M=10$). Using less than 10 coefficients results in r.m.s. errors of 0.17% for $M=9$, 0.24% for $M=8$, and 2.7% for $M=5$.

The correlated- k distribution method relies on the following approximations (Δm_j denotes the absorber column amount in, e.g., [molecules/cm²] corresponding to atmospheric layer j , ρ is the absorber concentration in, e.g., [molecules/cm³]):

$$\begin{aligned}
 \langle T_\lambda \rangle_{\Delta\lambda} &= \frac{1}{\Delta\lambda} \int_{\lambda_f}^{\lambda_t} \exp\left(-\int_0^{z_{max}} k_\lambda(z') \rho(z') dz'\right) d\lambda \approx \frac{1}{\Delta\lambda} \int_{\lambda_f}^{\lambda_t} \exp\left(-\sum_j^{N_z} k_{\lambda,j} \Delta m_j\right) d\lambda \\
 &\approx \int_0^1 \exp\left(-\sum_j^{N_z} k_{g,j} \Delta m_j\right) dg \approx \sum_{i=1}^M \omega_i \exp\left(-\sum_j^{N_z} k_{i,j} \Delta m_j\right). \quad (8)
 \end{aligned}$$

It is important to note that the number of terms M and weights ω_i are identical for all (N_z) layers for a given spectral interval; only the M pseudo cross-sections k_i are the parameters, which we fitted.

5.1.2. Overlapping line-absorbers

Overlapping line-absorbers have not been considered so far. In general, P overlapping absorbers might be considered by a *multivariate frequency distribution* Ω describing the probability that absorber m has cross-sections around $k_i^{(m)}$ and simultaneously (i.e. at the same wavelengths) absorber n has cross-sections around $k_j^{(n)}$ etc. in the wavelength interval of interest.²⁸ This means that ω_i has to be replaced by a P -dimensional quantity, like Ω_{ij} in case of $P=2$. Ω_{ij} might be interpreted as a cross-section correlation matrix. The mean transmittance for a homogeneous path may thus be approximated by

$$\langle T_\lambda(m_{(1)}, \dots, m_{(P)}) \rangle_{\Delta\lambda} \approx \sum_{i_{(1)}, \dots, i_{(P)}=1}^{M_{(1)}, \dots, M_{(P)}} \left[\Omega_{i_{(1)}, \dots, i_{(P)}} \exp\left(-\sum_{n=1}^P k_{i_{(n)}} m_{(n)}\right) \right]. \quad (9)$$

As in the 1-dimensional case the weights $\Omega_{i_{(1)}, \dots, i_{(P)}}$ have to be identical for all layers. In principle suitable weights for a each $\Delta\lambda$ might be defined along with representative ESFT coefficients as in the 1-dimensional case. In case of P absorbers and M coefficients per absorber this approach would require up to M^P RT calculations, i.e the computer time needed is in general much longer than in case of a single line-absorber.

If ESFT coefficients determined *independently* for each absorber (as described in subsection 5.2 below) shall be used for overlapping line-absorbers, it is necessary to assume a certain spectral correlation between the absorption cross-sections of individual line-absorbers.^{14 29} The advantage of this approach is that the non-linear fit does not have to deal with a large number of fit parameters which might cause problems especially due to the recognized

difficulties in fitting exponential sums.²⁷ The statistical approach, however, is also somewhat problematic, because the ESFT spectral intervals for this application are rather small, containing only a very limited number of lines.

A common approach is to assume that the transmittances/cross-sections of the individual line-absorbers are essentially *uncorrelated* within the wavelength interval of interest.¹⁴ In this case the mean transmittance of P overlapping gases can be calculated as the *product* of the mean transmittances of the individual absorbers resulting in $\Omega_{i(1), \dots, i(P)} = \omega_{i(1)} \dots \omega_{i(P)}$, i.e. the product of the individual weights. This approach, however, also requires M^P RT calculations rather than only M for the case of one absorber.

If the cross-sections were be perfectly *correlated*¹¹ the computer time would be similar to that for the one line-absorber only as in this case Ω_{ij} equals $\omega_i \delta_{ij}$, with δ_{ij} being the Kronecker symbol (i.e. $\delta_{ij} = 1$ if $i = j$, otherwise 0). This assumption seems, however, quite unrealistic and in most cases results in a significant overestimation of the transmittance/radiance.²⁹ However, the resulting error might be small in certain cases, e.g. if one strong line-absorber overlaps with other weak line-absorbers. Concerning the GOME spectral range the radiance error introduced by this approximation is rather small (less than about 1%) as the O₂ and H₂O bands are quite well separated below 790 nm. Similar remarks may hold for the assumption of perfect *anti-correlation* generally resulting in a significant underestimation of the radiance. In both of these extreme cases the computer time needed is essentially identical with the single line-absorber case.

Which fast approach actually lead to acceptable accuracy cannot be answered in general, but has to be determined for each spectral interval individually.

Between 240 and 1240 nm H₂O and O₂ are the only relevant line-absorbers (apart from a very weak CO₂ absorption around 1200 nm). The O₂ A-band around 760 nm is essentially free of H₂O absorption. Apart from this band and some very weak O₂ bands around 864 and 1068 nm, O₂ absorption is only significant in the γ - and B-bands around 630 and 690 nm, respectively, and these regions are relatively free of water absorption. This means that overlap of line-absorbers is only an issue for SCIAMACHY's channels 6-8 (1000-1750, 1940-2040, 2265-2380 nm, respectively). The most significant overlap in channel 6 is that of strong H₂O and CO₂ absorptions near 1435 nm. The results concerning this spectral range are presented in Section 6. Channels 7 and 8 clearly constitute a kind of worst case situation for the application of the c - k method, because in these channels the spectral resolution of SCIAMACHY is rather high ($\lambda/\Delta\lambda^{FWHM} \approx 10000$; $\Delta\bar{\nu}^{FWHM} \approx 0.35 \text{ cm}^{-1} \rightarrow \Delta\bar{\nu}^{ESFT} \approx 0.04 \text{ cm}^{-1}$ band model resolution), i.e. not too far from the LBL limit, and because there is a strong interference of the line-absorbers H₂O, CO₂, N₂O, and CO. The c - k method has not yet been applied in these channels.

5.2. Generation of ESFT data bases for GOMETRAN/SCIATRAN

Using the c - k (or ESFT) method it is possible to calculate the *mean* radiance or transmittances for a finite spectral interval much faster than using LBL calculations. However, even if these mean radiance calculations could be done without any error, this is not what is actually required for this application as neither GOME nor SCIAMACHY measure true spectral mean radiances due to the fact that the instrument's slit function is not an idealized box-car function.

The c - k approach actually corresponds to a box-car convolution of high resolution spectra subsequently sampled at the ESFT interval centre wavelengths. The actual instrument slit function is, however, bell-shaped (see Annex A) and has a FWHM on the order of two detector pixels. The approach followed here is to choose ESFT spectral intervals *smaller* than the instrument's spectral resolution FWHM and even smaller than the detector pixel resolution (about half of the resolution FWHM), i.e. on a wavelength grid finer than the measurement grid. c - k radiances calculated on this ESFT (i.e. sub-measurement) wavelength grid have finally to be convolved with an appropriate function and interpolated onto the instrument's wavelength grid if required. This convolution function, f^{ESFT} , might be defined by $f^{LBL} = f^{ESFT} \otimes f^{box-car}$, where f^{LBL} is the convolution function for the LBL spectra (i.e. the instrument's slit function), $f^{box-car}$ is a box-car function having a width corresponding to the ESFT averaging interval, and \otimes denotes convolution. As the selected ESFT intervals are small compared to the instrument's resolution (see also the note on wavelength interpolation in the next paragraph) $f^{ESFT} \approx f^{LBL}$ and this approximation has actually been used for the results presented in this paper.

The approach adopted here to use ESFT intervals smaller than the detector pixel resolution also helps to significantly reduce wavelength interpolation errors expected should the measurement wavelength grid differ from the ESFT grid (this will usually be the case when dealing with real measurements). Investigations in the O₂ A-band

region have shown that if c - k radiances would only be available on a wavelength grid with a spacing similar to the measurement grid the interpolation errors would exceed 1% in most cases even for small wavelength shifts.

For each ESFT spectral interval $\Delta\lambda$, each line-absorber, pressure, and temperature one set of M ESFT coefficients $k_i, i = 1 \dots M$, is determined by minimising the following expression

$$\sum_{n=1}^N \left[\langle T_\lambda(m_n) \rangle_{\Delta\lambda} - \sum_{i=1}^M \omega_i \exp(-k_i m_n) \right]^2 \rightarrow \min. \text{ w.r.t. } k_i. \quad (10)$$

$\langle T_\lambda(m_n) \rangle_{\Delta\lambda}$ is the reference mean transmittance obtained from LBL calculations. $m_n, n = 1 \dots N$, is the discretized column amounts array. These values are usually selected such that they cover a large range of column amounts [molecules/cm²], from a small fraction of one air mass up to several air masses, logarithmically sampled in order to cover several orders of magnitude of m values. This is important, as a large range of different optical path lengths are considered *simultaneously* in GT/ST: the radiation travels along several discrete stream angles, i.e. zenith angles with respect to the local vertical, from close to zero to close to 90°, in several different layers, having different concentrations and vertical extent, and, therefore, layer column amounts.

The ESFT weights ω_i are preselected. Several trials have shown, that Gaussian quadrature weights²² within the interval $[0, 1]$ seem to be a good choice. They automatically fulfill the requirement that their sum has to equal 1. In addition the smallest values occur at $i = 1$ and $i = M$ and the largest values are in the middle of the interval. This corresponds quite well with the usual g dependence of the k distribution k_g having the strongest (positive) derivative w.r.t. g near $g = 0$ and $g = 1$ and being generally quite flat in the middle of the g interval.

Fitting exponential sums (like ESFT) is known to be a classical *ill conditioned* problem of numerical analysis.²⁷ ESFT is slow, stops often far from the correct minimum (even with a good initial guess), is instable, i.e. even small variations of the function being fitted leads to large variations in the fit parameters, and often produces negative results. Tests with a standard NLLS Levenberg-Marquardt algorithm²² have shown, that at least one negative pseudo cross-section results in 10-20% of all cases. This problem has been dealt with by using a NLLS fitting methods that enables constraints to be placed on all fit parameters. For this purpose subroutine E04NAF from the NAG FORTRAN library³⁰ has been selected. This routine solves the so called quadratic programming (QP) problem^{30 31}:

$$\text{minimize } \bar{c}^T \bar{x} + \frac{1}{2} \bar{x}^T H \bar{x} \quad \text{w.r.t. } \bar{x} \in R^n \quad \text{subject to } \begin{pmatrix} \bar{x} \\ C\bar{x} \end{pmatrix} \leq \bar{u}. \quad (11)$$

\bar{c} is a constant vector of order n (= number of fit parameters) and H is a constant n by n symmetrical matrix. The constraints matrix C is of order m by n , where m may be zero. m is the number of constraints on linear combinations of the fit parameters in addition to the n constraints that can be placed on the fit parameters directly. Vectors \bar{l} and \bar{u} are the lower and upper boundary constraints on \bar{x} and $C\bar{x}$.

In order to use this routine the ESFT problem has been transformed into the corresponding QP problem. For this purpose the non-linear ESFT problem had to be linearized. Starting from first guess coefficients, E04NAF is called several times during the iteration.

First guess ESFT coefficients are obtained by solving a *linear* least squares problem for each Δg_i interval separately. The first guess coefficients \hat{k}_i^o are obtained requiring

$$\langle T_g(m) \rangle_{\Delta g_i} := \frac{1}{\omega_i} \int_{\Delta g_i} \exp(-k_g m) dg \approx \exp(-\hat{k}_i^o m). \quad (12)$$

Solving this problem for the predefined set of m values yields, after taking the logarithm and applying the linear least squares minimization:

$$\hat{k}_i^o = \frac{-\sum_{j=1}^N \ln(\langle T_g(m_j) \rangle_{\Delta g_i}) m_j}{\sum_{j=1}^N m_j^2}. \quad (13)$$

The ESFT problem might be written in the following notation:

$$\left(\vec{L} - \vec{E}(\vec{k})\right)^T \left(\vec{L} - \vec{E}(\vec{k})\right) \rightarrow \min. \text{ w.r.t. } \vec{k}. \quad (14)$$

\vec{E} denotes the ESFT-sum vector (each element for a different m_j) and \vec{L} the reference mean LBL transmittance w.r.t. the wavelength interval of interest, $\Delta\lambda$. T denotes transposed.

Linearization of $\vec{E}(\vec{k})$ at \vec{k}_o (first guess fit parameter vector at the beginning of the iteration or latest guess during the iteration) results in

$$\vec{E}(\vec{k}) \approx \vec{E}(\vec{k}_o) + \frac{\partial \vec{E}(\vec{k}_o)}{\partial \vec{k}} \Delta \vec{k}. \quad (15)$$

With $\Delta \vec{k} := \vec{k} - \vec{k}_o$, matrix $A := \partial \vec{E}(\vec{k}_o) / \partial \vec{k}$, and $\vec{y} := \vec{L} - \vec{E}(\vec{k}_o)$ the following equation can be derived

$$-(A^T \vec{y})^T \Delta \vec{k} + \frac{1}{2} \Delta \vec{k}^T A^T A \Delta \vec{k} \rightarrow \min. \text{ w.r.t. } \Delta \vec{k}. \quad (16)$$

This equation already has the desired QP form. The following quantities can be identified:

$$\vec{c} := -(A^T \vec{y})^T, \quad \vec{x} := \Delta \vec{k}, \quad H := A^T A. \quad (17)$$

Matrix A can be derived analytically: $A_{ij} = -\omega_j m_i \exp(-k_j m_i)$. The constraints have been implemented such that each fit parameter k_i can only be doubled or reduced by 50% at maximum. This assures that starting with positive first guess values, all parameters might be subject to change during the iteration and still stay positive. The iteration stops when the relative change of the *r.m.s.* difference between the ESFT and the LBL transmittance is essentially constant, or if a predefined maximum number of iterations is reached.

Before and after the NLLS fit the *average* relative error ($\sum_i |E_i - L_i| / L_i * 100$) as well as the *maximum* relative error ($\{|E_i - L_i| / L_i * 100\}_{max}$) is determined. If the average or the maximum error obtained with the first guess coefficients turns out to be less than the corresponding errors after the fit, the first guess coefficients are used instead of the NLLS coefficients. Thus the fit is expected also to improve the maximum deviation (which is usually the case). If the transmittances are rather small (e.g. less than 1%) the corresponding points are excluded from the error calculation because the absolute transmittance error is small under these circumstances.

5.3. Implementation of the ESFT approach in GOMETRAN/SCIATRAN

ESFT coefficients have been generated for ten pressures and six temperatures including extreme atmospheric values. The ESFT coefficients for the actual atmospheric height grid are obtained by bi-linear interpolation from the tabulated ESFT data base values. If pressure or temperature extrapolation is required the nearest ESFT coefficients stored in the data base are used.

6. COMPARISON OF LBL AND C-K TRANSMITTANCES AND RADIANCES

The *c-k* radiances have been compared with simulated SCIAMACHY and GOME radiance spectra. These reference spectra are high-resolution (LBL) *sun-normalised* radiance spectra, i.e. earthshine radiance divided by solar irradiance, convolved with an appropriate instrument slit function and sampled according to the instrument wavelength grid. Strictly speaking, GOME and SCIAMACHY do not measure convolved *sun-normalised* radiances but convolved earthshine radiance and convolved solar irradiance separately. Since the solar spectrum is rather flat for wavelength larger than about 600 nm, where strong line absorptions occur, the approach to use *sun-normalised* radiance spectra should be sufficient.

The following error values refer to an ESFT spectral interval of about one quarter of the detector pixel resolution (0.05 nm in channels 3 and 4) corresponding to about 1/8 of the spectral resolution and to $M = 5$ coefficients. This error can be significantly reduced by increasing M , but this would, of course, increase the computer time as well.

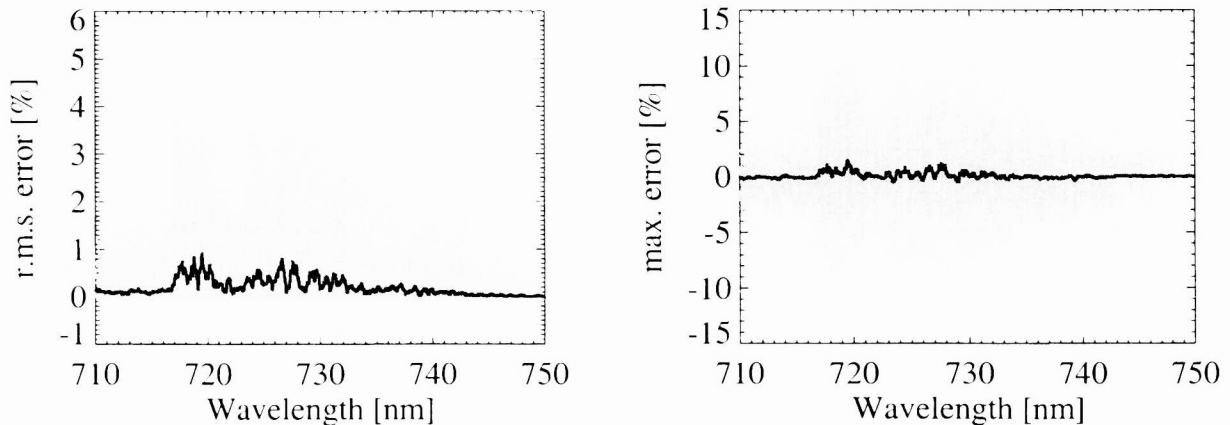


Figure 2. ESFT transmittance fit errors for the H_2O band around 720 nm for 48000 scenarios (800 ESFT spectral intervals (0.05 nm each) times 10 pressures times 6 temperatures) for $M=5$ coefficients (grey dots). The black curve is obtained after box-car convolution. The box-width corresponds to the spectral resolution FWHM of this channel (0.35 nm). In 95% of all cases the (not averaged) r.m.s. error (left) is less than 1% (78% < 0.2%, 98% < 2%). The absolute value of the maximum error (right) is less than 3% in 93% of all 48000 cases (78% < 1%, 88% < 2%).

The *r.m.s.* and the similarly defined *average* transmittance errors are less than 1% in about 90% and less than 3% in about 99% of all cases (different line-absorbers, wavelengths, pressures, and temperatures). If these errors are averaged according to the instrument's resolution they are reduced to about 1% (see Figure 2). The absolute value of the *maximum* transmittance error is less than about 3% in about 90% of all cases and less than about 10% in essentially all cases. If the maximum errors are averaged according to the instrument's resolution the error is reduced to about $\pm 1\%$.

The radiance error *after* slit function convolution (this is the most important value characterising the impact of *c-k* errors on the retrieval), i.e. the end-to-end difference between the *c-k* and the reference LBL radiance, is less than 1% in most cases and less than 2% for all situations investigated so far (see Figure 3). The mean radiance error w.r.t. the ESFT averaging intervals (comparison with *mean* LBL radiances, i.e. averaged for each ESFT interval without slit function convolution) is less than $\pm 6\%$. This error is reduced to generally less than $\pm 1\%$ by the convolution process. These values hold for all scenarios investigated so far, e.g. covering the relevant solar zenith angle range of about 20° - 92° . For weak line-absorption the corresponding errors are significantly smaller. For example the radiance error is less than about 0.06% for the water bands around 504 nm.

As already mentioned earlier the spectral region with the strongest overlap of line-absorbers in SCIAMACHY's channels 1-6 is located around 1435 nm due to strong overlapping H_2O and CO_2 absorption bands. ESFT coefficients for both absorbers have been generated for each molecule independently, similar as for the H_2O and O_2 bands already discussed (i.e. $M = 5$ coefficients, ESFT spectral intervals about 1/8 of the spectral resolution (1.6 nm / 8 = 0.2 nm)). As for the strong H_2O and O_2 bands the agreement w.r.t. LBL calculations is within ± 1 -2% for the convolved radiances in case only one absorber is present.

In order to model both absorbers simultaneously in GT/ST several commonly made statistical assumptions concerning the correlation of the individual transmittances / absorption cross-sections as described in subsection 5.1.2 have been tested. The most commonly used assumption of *uncorrelated* transmittances (or absorption cross-sections) leads to unacceptable radiance errors (difference ESFT - LBL radiance after convolution) of up to $\pm 10\%$. This is mainly related to the fact that the average distance between the CO_2 lines in this spectral region is about 0.4 nm resulting in just one line (if any) per 0.2 nm ESFT interval. If the spectral averaging interval would cover the complete CO_2 band this error would be much smaller. The assumption of (*positive*) *correlation*, see subsection 5.1.2, results in errors up to +20% (systematic overestimation) and the *anti-correlation* assumption results in errors up to -30% (systematic underestimation).

A very promising accurate and fast approach is based on a *linear combination* of radiances calculated assuming positive and negative (i.e. anti-) correlation of the cross-sections, I^{+corr} and I^{-corr} , respectively. I_i^{+corr} is calculated using cross-section combination $\{k_i^{H_2O}, k_i^{CO_2}\}$, i.e. the weakest H_2O pseudo cross-section is combined with the weakest

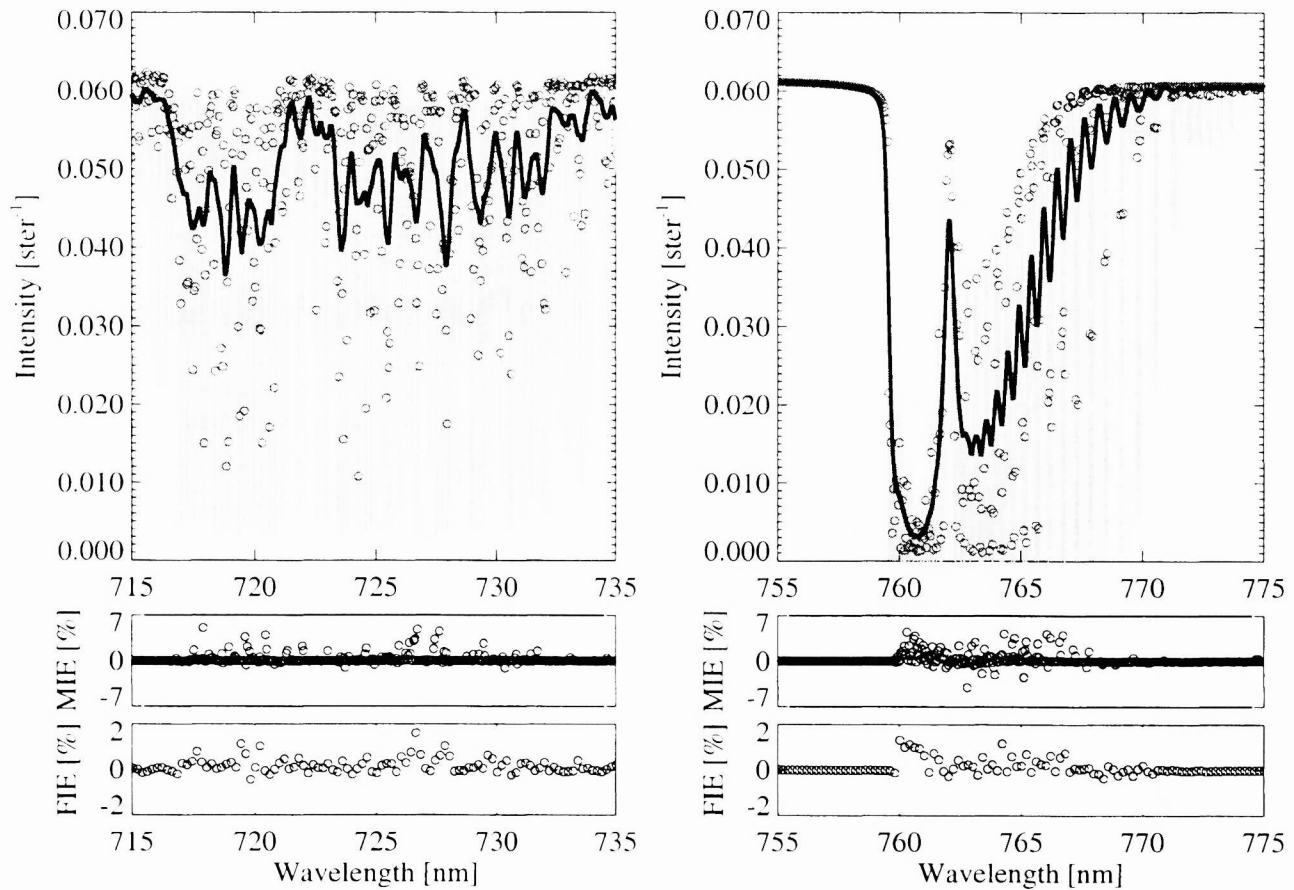


Figure 3. Left: Top: top-of-atmosphere intensities for nadir viewing geometry in the 720 nm spectral region dominated by strong line-absorption due to water vapour. The intensity is defined as the sun-normalised radiance for a solar flux of π . Scenario: US standard atmosphere, multiple scattering, solar zenith angle 60° , albedo 10%, and maritime / stratospheric background aerosol. LBL intensities (thin grey lines), *c-k* intensities without convolution for ESFT intervals of 0.05 nm (circles), and convolved LBL and *c-k* intensities (slit function FWHM 0.35 nm) shown as black solid lines (essentially one line on this scale). Middle: relative difference (MIE = Mean Intensity Error) between *c-k* and LBL mean intensities for each 0.05 nm ESFT interval (without slit function convolution). Bottom: end-to-end *c-k* - LBL Final Intensity Error (FIE) after slit function convolution. The maximum deviation between GOMETRAN/SCIATRAN intensities calculated in *c-k* and in LBL mode is about 1.5%. The *c-k* mode is about a factor of 60 faster than the LBL mode. Right: same as on left side but for the O_2 A-band around 720 nm.

O_2 pseudo cross-section etc., and I_i^{-corr} using $\{k_i^{H_2O}, k_{M+1-i}^{CO_2}\}$, i.e. the weakest H_2O pseudo cross-section is combined with the strongest pseudo cross-section of O_2 etc. (for each height level, i.e. pressure and temperature). The mean radiance for each ESFT spectral interval is determined from $2M$ RT calculations only rather than from about M^2 calculations in the general case or in case of uncorrelated cross-sections (see also Equation 7):

$$\langle I \rangle_{\Delta\lambda}^{c-k} = \sum_{i=1}^M (\alpha \omega_i I_i^{+corr} + (1 - \alpha) \omega_i I_i^{-corr}). \quad (18)$$

Mixing parameter α has been determined for each ESFT spectral interval $\Delta\lambda$ individually by matching the *c-k* radiance to the mean LBL reference radiance for a certain (“representative”) atmospheric scenario, solar zenith angle, and viewing geometry, i.e.

$$\langle I \rangle_{\Delta\lambda}^{LBL} =: \alpha \langle I \rangle_{\Delta\lambda}^{+corr} + (1 - \alpha) \langle I \rangle_{\Delta\lambda}^{-corr}. \quad (19)$$

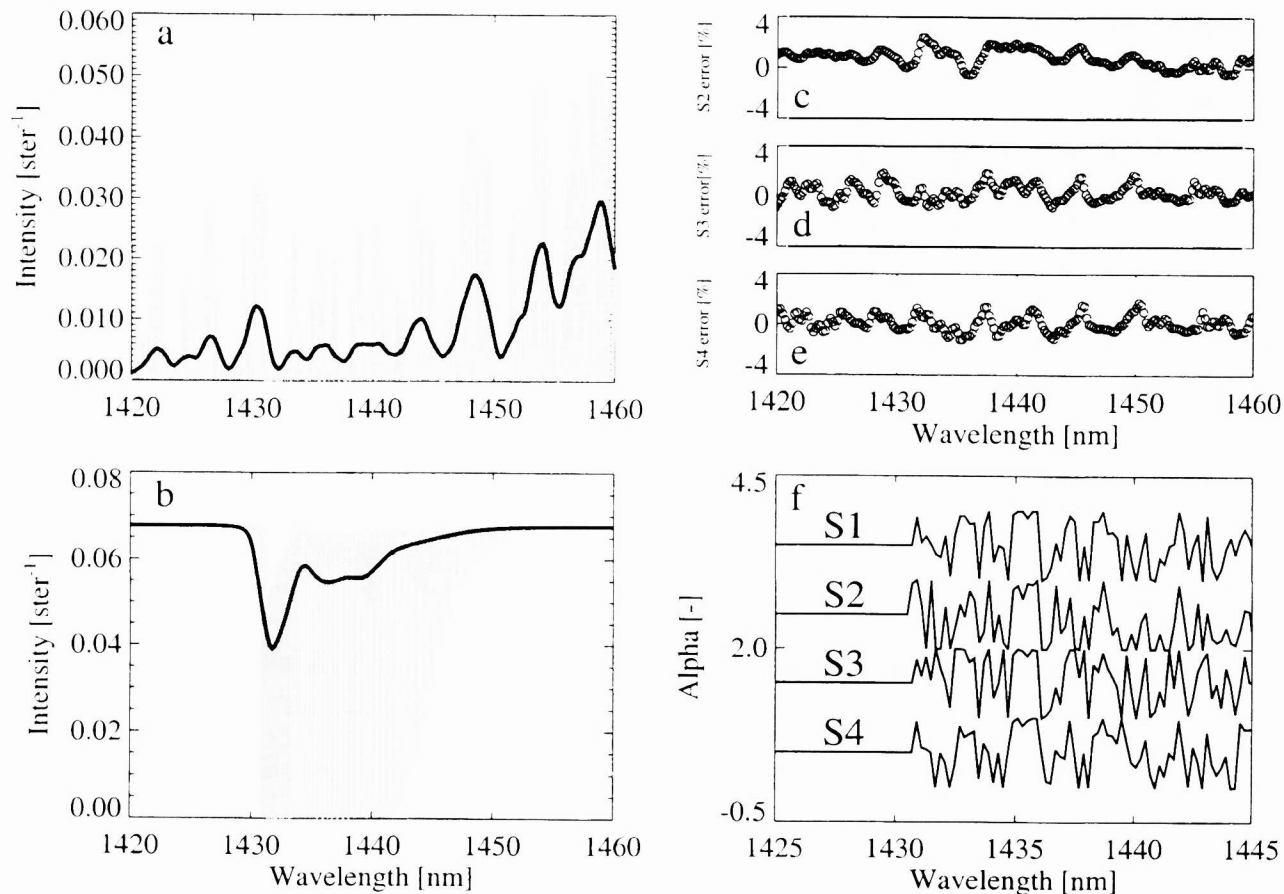


Figure 4. (a) LBL intensity (thin grey line) and convolved intensity (thick dark line; slit function FWHM 1.6 nm) in the 1435 nm spectral region for scenario S1 dominated by strong overlapping H₂O and CO₂ absorption. (b) As (a) but for CO₂ absorption only. Panels (c)-(e) are showing the relative difference between c-k and LBL radiances for scenarios S2-S4 with α determined from S1. Panel (f) shows mixing parameter α for all four scenarios (with offsets for clarity).

Thus mixing parameter $\alpha := (\langle I \rangle_{\Delta\lambda}^{-corr} - \langle I \rangle_{\Delta\lambda}^{LBL}) / (\langle I \rangle_{\Delta\lambda}^{+corr} - \langle I \rangle_{\Delta\lambda}^{-corr})$. If $\alpha < 0$ or $\alpha > 1$, α has been set to 0 or 1, respectively. If the denominator is close to zero, i.e. if the radiances are identical within 0.5%, α has been set to 0.5. This approach, of course, leads to very small radiance errors provided the atmospheric scenario, the solar zenith angle (SZA), and the viewing geometry are similar to the scenario used for the determination of α . As α should mainly express how the monochromatic H₂O and CO₂ cross-sections are correlated (e.g. α should be close to 1 in case of positive correlation and close to 0 in case of anti-correlation) α is expected to depend only weakly on the scenario selected for the determination of α . In order to check the quality of α four rather different scenarios (S1-S4) have been defined. For each of these scenarios c-k radiances have been compared with corresponding LBL radiances using a single α determined from one scenario only (S1). Scenarios S1-S4 have been defined as follows (common parameters: albedo 10%, multiple scattering, maritime / stratospheric background aerosol):

Scenario ID	Atmosphere	SZA	Viewing geometry
S1	US standard atmosphere	50°	nadir view from satellite
S2	US standard atmosphere	88°	nadir view from satellite
S3	US standard atmosphere	50°	zenith view from surface
S4	Tropical atmosphere	20°	nadir view from satellite

Figure 4 shows the results achieved using this mixing method of treating overlapping line-absorbers. It can be seen that the different α determined independently for scenarios S1-S4 correlate quite well as expected (panel *f*). Panels *c-e* show that the *c-k* and LBL radiances agree within 1-3% for scenarios S2-S4 even though α was only derived from S1.

The *c-k* mode is significantly faster than the LBL mode for two reasons. First, the RT matrix equation needs to be solved less times in *c-k* mode than in LBL mode. E.g. in channels 3 and 4 (400-800 nm) the RT equation has to be solved 5 times (assuming $M = 5$ ESFT coefficients) for each 0.05 nm ESFT interval and about 100 (= 0.05/0.0005) times in LBL mode for the same interval assuming a spectral sampling of 0.0005 nm (corresponding to 0.008 cm^{-1} at 760 nm). This means that the *c-k* mode is at least 20 times faster in this spectral region. For channel 6 *c-k* calculations are even a factor of 80 faster (single line-absorber case) due to the four times lower spectral resolution (i.e. larger FWHM). Second, the LBL mode requires rather time consuming absorption cross-section calculations (Voigt line shape) whereas the corresponding ESFT coefficients for the *c-k* mode have been precalculated. In principle, it would also be possible to precalculate the monochromatic absorption cross-sections needed for the LBL calculations but this would require a huge storage space. However, this might be a reasonable approach for selected spectral micro-windows. In total the presently implemented *c-k* mode is a factor of about 60 times faster than the LBL mode in the 720 nm spectral region (H_2O), a factor of 25 in the O_2 A-band region around 760 nm, and a factor of about 800 faster in the 1000-1750 nm region corresponding to SCIAMACHY's channel 6 in case of a single line-absorber and a factor of about 400 in case of two overlapping line-absorbers.

7. COMPARISON WITH MODTRAN/DISORT

Concerning the final end-to-end validation of the *c-k*/ESFT implementation in GT/ST w.r.t. an independent RT model, GT/ST spectra have been compared with radiances calculated with MODTRAN3.7 V1.0¹⁶ using the DISORT multiple scattering option.¹⁷ Good agreement has been found (see Figure 5). Minor differences on the order of a few percent are probably due to different band model resolution and details of the convolution process. Note that the resolution of the MODTRAN band model is 1 cm^{-1} corresponding to 0.052/0.058 nm at 720/760 nm. This means that the MODTRAN band model resolution is close to but not equal with the GT/ST band model resolution in the regions of the H_2O and O_2 bands presented in this paper. Figure 5 shows that the up to 2.5% deviation between GT/ST and MODTRAN in the 720 nm spectral region cannot be explained by the GT/ST *c-k* scheme as the GT/ST *c-k* - LBL differences are significantly smaller.

8. CONCLUSIONS

For radiative transfer modeling of line-absorbers like O_2 , H_2O , CO_2 , CH_4 , N_2O , and CO in the UV-Vis-NIR spectral range covered by SCIAMACHY (240-2380 nm) with the multiple scattering radiative transfer code GOME-TRAN/SCIATRAN two schemes have been implemented and compared. First a straightforward line-by-line (LBL) scheme which has been implemented mainly for reference purposes and second a fast correlated-*k* distribution (*c-k*) band model scheme optimized for retrieval from GOME and SCIAMACHY data. Detailed results for three spectral regions have been presented: the 720 nm region dominated by strong H_2O absorption, the 760 nm O_2 A-band region and the 1435 nm region dominated by strong overlapping H_2O and CO_2 absorption. For a single line-absorber simulated GOME and SCIAMACHY top-of-atmosphere radiances calculated with both methods agree within ± 1 -2% even in case of strong absorptions for all scenarios investigated so far, e.g. covering the relevant solar zenith angle range 20° - 92° ; the agreement is much better for weak absorption bands. The *c-k* mode is a factor of 25-800 faster than the LBL mode depending on spectral interval. Agreement within a few percent has been found when comparing *c-k* and LBL radiances with the MODTRAN/DISORT radiative transfer model in the 700-800 nm spectral region where the band model resolutions are similar. First results have been presented concerning spectral regions with overlapping line absorbers. A new method has been presented that combines individually determined *c-k* coefficients such that essentially the same accuracy w.r.t. LBL results can be achieved as in the single line-absorber case with only a factor of two increase in computer time compared to the one absorber case.

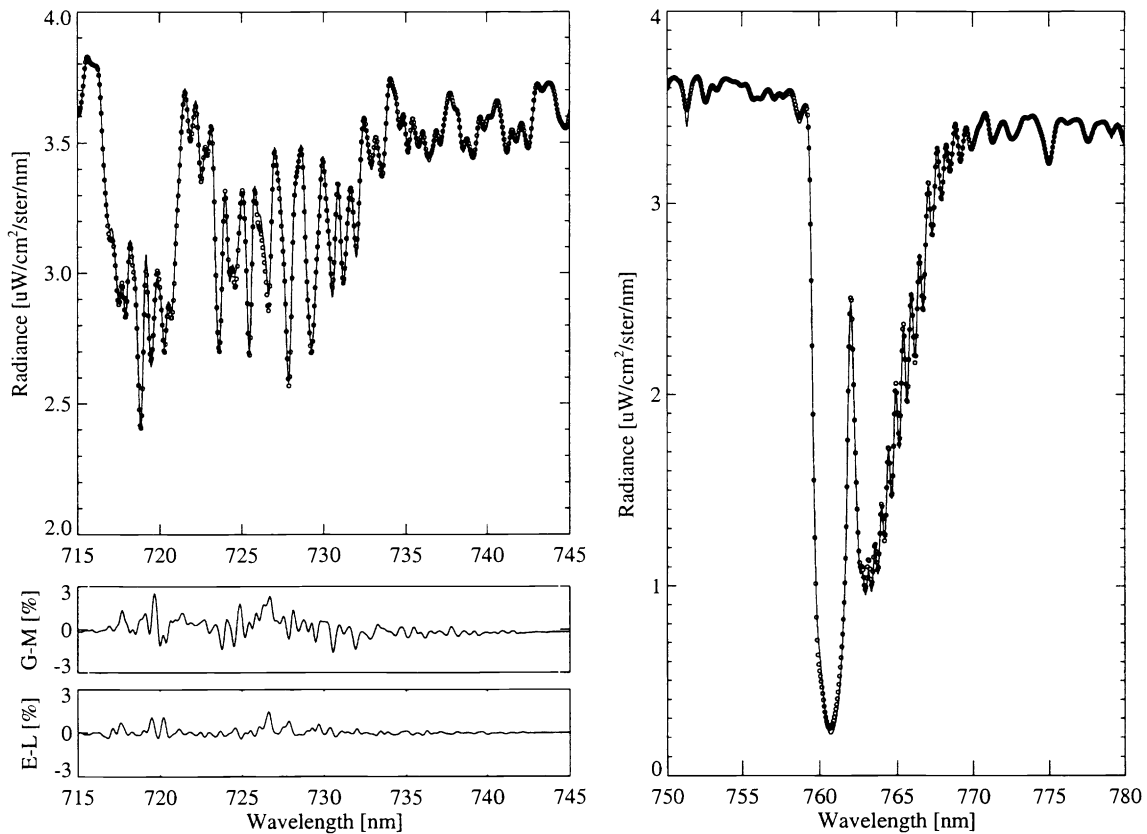


Figure 5. Left: Top: GOMETRAN/SCIATRAN top-of-atmosphere *c-k* radiance (solid line) and MODTRAN/DISORT radiance (circles) in the 720 nm spectral region dominated by strong H₂O absorption. Scenario as for Figure 3 but for a solar zenith angle of 30° (solar spectrum from MODTRAN; convolution with Gaussian slit function (FWHM 0.35 nm)). Middle: relative difference between GT/ST and MODTRAN/DISORT after linear interpolation on GT/ST wavelength grid. Bottom: Relative difference between GT/ST in *c-k* and in LBL mode. Right: similar as top of left side but for the spectral region of the O₂ A-band.

APPENDIX A. SLIT FUNCTIONS

The following two SCIAMACHY and GOME like (analytical) slit functions have been used in order to generate the simulated measurements:

A “simple hyperbolic” slit function (default)

$$f^{hyp}(\lambda - \lambda_o) = \frac{1}{16 \left(\frac{\lambda - \lambda_o}{\delta\lambda} \right)^4 + 1} \quad (20)$$

and a Gaussian slit function (for comparison with MODTRAN)

$$f^{gau}(\lambda - \lambda_o) = \exp \left(- \left(\sqrt{\ln 2} \frac{2(\lambda - \lambda_o)}{\delta\lambda} \right)^2 \right). \quad (21)$$

λ denotes wavelength, λ_o the center wavelength, and $\delta\lambda$ denotes the full-width at half-maximum in wavelength units (usually [nm]). Both functions are normalized to unity at center wavelength.

ACKNOWLEDGMENTS

This work has been funded as part of the SCIAMACHY Scientific Support Study by the German ministry for science, technology and education BMBF (formerly represented by the German Space Agency DARA, now DLR) grant 50EP9207 and the University of Bremen.

REFERENCES

1. J. P. Burrows, E. Hölzle, A. P. H. Goede, H. Visser, and W. Fricke, "SCIAMACHY - SCanning Imaging Absorption spectroMeter for Atmospheric CHartographY," *Acta Astronautica* **35** (7), pp. 445–451, 1995.
2. H. Bovensmann, J. P. Burrows, M. Buchwitz, J. Frerik, S. Noël, V. V. Rozanov, K. V. Chance, and A. Goede, "SCIAMACHY - mission objectives and measurement modes." *J. Atmos. Sci.* (in press), 1998.
3. J. P. Burrows, M. Weber, M. Buchwitz, V. V. Rozanov, A. Ladstätter-Weißmayer, A. Richter, R. de Beek, R. Hoogen, K. Bramstedt, K.-U. Eichmann, and M. Eisinger, "The Global Ozone Monitoring Experiment (GOME): Mission concept and first scientific results." *J. Atmos. Sci.* (in press), 1998.
4. V. V. Rozanov, D. Diebel, R. J. D. Spurr, and J. P. Burrows, "GOMETRAN: A radiative transfer model for the satellite project GOME - the plane-parallel version," *J. Geophys. Res.* **102** (D14), pp. 16.683–16.695, 1997.
5. V. V. Rozanov, T. Kurosu, and J. P. Burrows, "Retrieval of atmospheric constituents in the UV-visible: A new quasi-analytical approach for the calculation of weighting functions," *J. Quant. Spectrosc. Radiat. Transfer* **60** (2), pp. 277–299, 1998.
6. C. Blindauer, V. V. Rozanov, and J. P. Burrows, "Actinic flux and photolysis frequency comparison computations using the model PHOTOGT," *Journal of Atmospheric Chemistry* **24**, pp. 1–21, 1996.
7. T. Kurosu, V. V. Rozanov, and J. P. Burrows, "Parameterization schemes for terrestrial water clouds in the radiative transfer model GOMETRAN," *J. Geophys. Res.* **102** (D18), pp. 21.809–21.823, 1997.
8. P. Köpke, A. Bais, D. Balis, M. Buchwitz, and H. D. B. et al., "Comparison of models used for UV index calculations." *Photochemistry and Photobiology* (in press), 1998.
9. M. Vountas, V. V. Rozanov, and J. P. Burrows, "Ring effect: Impact of rotational Raman scattering on radiative transfer in Earth's atmosphere." *J. Quant. Spectrosc. Radiat. Transfer* (in press), 1998.
10. R. Hoogen, V. V. Rozanov, and J. P. Burrows, "Ozone profiles from GOME satellite data: Algorithm description and first validation." submitted to *J. Geophys. Res.*, 1998.
11. R. G. Isaacs, W.-C. Wang, R. D. Worsham, and S. Goldenberg, "Multiple scattering LOWTRAN and FASCODE models," *Applied Optics* **26** (7), pp. 1272 – 1281, 1997.
12. R. M. Goody and Y. L. Yung, *Atmospheric Radiation - Theoretical Basis*, Oxford University Press, Oxford, UK, 1989.
13. R. M. Goody, R. West, L. Chen, and D. Crisp, "The correlated-k method for radiation calculations in nonhomogeneous atmospheres," *J. Quant. Spectrosc. Radiat. Transfer* **42** (6), pp. 539–550, 1989.
14. A. A. Lacis and V. Oinas, "A description of the correlated k distribution method for modeling nongray gaseous absorption, thermal emission, and multiple scattering in vertically inhomogeneous atmospheres," *J. Geophys. Res.* **96** (D5), pp. 9027–9063, 1991.
15. A. Kuze and K. V. Chance, "Analysis of cloud top height and cloud coverage from satellite using O₂ A and B bands," *J. Geophys. Res.* **99**, pp. 14481–14491, 1994.
16. K. Stamnes, S.-C. Tsay, and M. Yeh, "Upgrade of FASCODE and MODTRAN to full solar capability including multiple scattering and spherical geometry," tech. rep., Draft Final Report to PL/Geophysics Directorate, 1994.
17. K. Stamnes, S.-C. Tsay, W. Wiscombe, and K. Jayaweera, "Numerically stable algorithm for discrete-ordinate-method radiative transfer in multiple scattering and emitting layered media," *Appl. Optics* **27** (12), pp. 2502–2509, 1988.
18. A. Dahlback and K. Stamnes, "A new spherical model for computing the radiation field available for photolysis and heating at twilight," *Planet. Space Sci.* **39** (5), pp. 671–683, 1991.
19. M. Weber, J. P. Burrows, and R. P. Cebula, "GOME solar UV/Vis irradiance measurements between 1995 and 1997 - first results on proxy solar activity studies," *Solar Physics* **177**, pp. 63–77, 1998.
20. H. Schrijver, S. Slijkhuis, M. G. M. Römer, and A. P. H. Goede, "Noise related limits on the detectability of concentration variations of CH₄ and CO with SCIAMACHY," in *Atmospheric Sensing and Modeling*, R. P. Santer, ed., *Proc. SPIE* **2311**, pp. 39–46, 1995.

21. H. Schrijver, A. P. H. Goede, M. R. Dobber, and M. Buchwitz, "Retrieval of carbon monoxide, methane and nitrous oxide from SCIAMACHY measurements." submitted to *Proc. SPIE*, Beijing, China, 14-17 Sept, 1998.
22. W. H. Press, S. A. Teukolsky, W. T. Vetterling, and B. P. Flannery, *Numerical Recipes in FORTRAN - The Art of Scientific Computing*, Cambridge University Press, Cambridge, UK, 1992.
23. T. R. Caudill, D. E. Flittner, B. M. Herman, O. Torres, and R. D. McPeters, "Evaluation of the pseudo-spherical approximation for backscattered ultraviolet radiances and ozone retrieval," *J. Geophys. Res.* **102 (D3)**, pp. 3881-3890, 1997.
24. K. X. Kneizys, E. P. Shettle, L. W. Abreu, J. H. Chetwynd, G. P. Anderson, W. O. Gallery, J. E. A. Selby, and S. A. Clough, "Users guide to LOWTRAN 7," tech. rep., Air Force Geophys. Lab., 1988.
25. L. S. Rothman, R. R. Gamache, R. H. Tipping, C. P. Rinsland, M. A. H. Smith, D. C. Benner, V. M. Devi, J.-M. Flaud, C. Camy-Peyret, A. Perrin, A. Goldman, S. T. Massie, L. R. Brown, and R. A. Toth, "The HITRAN molecular database: Editions of 1991 and 1992," *J. Quant. Spectrosc. Radiat. Transfer* **48 (5)**, pp. 469-507, 1992.
26. J. Humlicek *J. Quant. Spectrosc. Radiat. Transfer* **27**, p. 437, 1982.
27. W. J. Wiscombe and J. W. Evans, "Exponential-sum fitting of radiative transmittance functions," *Journal of Computational Physics* **24**, pp. 416-444, 1977.
28. H.-D. Hollweg, "A k distribution method considering centres and wings of atmospheric absorption lines," *J. Geophys. Res.* **98 (D2)**, pp. 2747-2756, 1993.
29. K. M. Firsov, A. A. Mitsel, Y. N. Ponomarev, and I. V. Ptashnik, "Parameterisation of transmittance for application in atmospheric optics," *J. Quant. Spectros. Radiat. Transfer* **59**, pp. 203-213, 1998.
30. "NAG Fortran Library Manual, Mark 15," Oxford, UK, 1991. NAG (Numerical Algorithm Group) Ltd.
31. P. E. Gill and W. Murray, *Practical Optimisation*, Academic Press, London, UK, 1981.